Observation of Periodic Fine Structure in Reflectance from Biological Tissue: A New Technique for Measuring Nuclear Size Distribution

L. T. Perelman,[1] V. Backman,[1] M. Wallace,[2] G. Zonios,[1] R. Manoharan,[1] A. Nusrat,[3] S. Shields,[4] M. Seiler,[4] C. Lima,[1] T. Hamano,[1] I. Itzkan,[1] J. Van Dam,[2] J. M. Crawford,[5] and M. S. Feld[1]

[1]*G. R. Harrison Spectroscopy Laboratory, Massachusetts Institute of Technology, Cambridge, Massachusetts 02139*

[2]*Gastroenterology Division, Brigham and Women's Hospital, Boston, Massachusetts 02115*

[3]*Department of Pathology, Brigham and Women's Hospital, Boston, Massachusetts 02115*

[4]*U.S. Veterans Hospital, West Roxbury, Massachusetts 02132*

[5]*Department of Pathology, Yale University School of Medicine, New Haven, Connecticut 06520-8023*

(Received 9 July 1997)

We report observation of a fine structure component in backscattered light from mucosal tissue which is periodic in wavelength. This structure is ordinarily masked by a diffusive background. We have identified the origin of this component as being due to light which is Mie scattered by surface epithelial cell nuclei. By analyzing the amplitude and frequency of the fine structure, the density and size distribution of these nuclei can be extracted. These quantities are important indicators of neoplastic precancerous changes in biological tissue. [S0031-9007(97)05049-7]

PACS numbers: 87.64.–t, 42.62.Be, 87.64.Ni

Biological tissue is a turbid optical medium, in which light transport is dominated by elastic scattering [1–3]. The primary scattering centers are thought to be the collagen fiber network of the extracellular matrix, the mitochondria, and other intracellular substructures, all with dimensions smaller than optical wavelengths [3]. However, larger structures, such as cell nuclei, typically 5–15 μm in diameter, can also scatter light.

Single scattering of collimated light is used widely to study cells and subcellular structures in suspension [4]. This approach cannot be used in tissue, since light is then randomized by multiple scattering. Nevertheless, diffusely scattered light from tissue contains information about its underlying structures [5]. Both transmitted [6] and backscattered [7] photons can be used to measure particle size. However, because of randomization, this information is averaged over several transport lengths. On the other hand, the light in the thin layer at the tissue surface is not completely randomized and information about individual scatterers can be retained, even if the layer thickness is significantly smaller than a transport length. In this Letter, we exploit this fact to extract the density and size distribution of cell nuclei near the tissue surface.

Mucosal tissues, which line the hollow organs of the body, generally consist of a thin surface layer of epithelial cells supported by underlying, relatively acellular connective tissue. In healthy tissues, the epithelium often consists of a single, well-organized layer of cells with the diameter of 10–20 μm and the height of 25 μm. In cancerous and precancerous (dysplastic) epithelium, the cells proliferate and the cell nuclei enlarge and appear darker (hyperchromatic) when stained [8].

Epithelial nuclei are spheroidal Mie scatterers with refractive index higher than that of the surrounding cytoplasm [9,10]. Normal nuclei have a characteristic diameter $l = 4$–7 μm. In contrast, dysplastic nuclei can be as large as 20 μm in height, occupying almost the entire cell volume. In the visible range, the wavelength $\lambda \ll l$ and the Van de Hulst approximation [11] can be used to describe the optical scattering cross section of the nuclei:

$$\sigma_s(\lambda, l) = \frac{1}{2}\pi l^2\left[1 - \frac{\sin(2\delta/\lambda)}{\delta/\lambda} + \left(\frac{\sin(\delta/\lambda)}{\delta/\lambda}\right)^2\right], \tag{1}$$

where $\delta = \pi l n_c(n - 1)$, where n_c is the refractive index of cytoplasm and n is the refractive index of the nuclei relative to that of cytoplasm. Thus, the scattering cross section of the nuclei exhibits a periodicity with wavelength [12]. As shown below, this gives rise to a periodic component in the reflectance from the tissue.

Consider a beam of light incident on an epithelial layer of tissue. A portion of this light is backscattered from the epithelial nuclei, while the remainder is transmitted to deeper tissue layers, where it undergoes multiple scattering and becomes randomized. All of the diffusive light which is not absorbed in the tissue eventually returns to the surface, passing once more through the epithelium, where it is again subject to scattering from the cell nuclei. Thus, the emerging light will consist of a large diffusive background plus the component of forward scattered and backscattered light from the nuclei in the epithelial layer. For a thin slab of epithelial tissue containing nuclei with size distribution $N(l)$ [number of nuclei per unit area (mm^2) and per unit interval of nuclear diameter (μm)], the approximate solution of the transport equation for the reflectance $R(\lambda)$ collected by an optical probe with acceptance solid angle Ω_c is given by the following

expression:

$$\frac{R(\lambda)}{\overline{R}(\lambda)} = e^{-\tau(\lambda)} + \frac{1 - e^{-\tau(\lambda)}}{\langle I_d(\lambda, \mathbf{s})\rangle_{\Omega_c}} \times \langle\langle I_i(\lambda, -\mathbf{s}')p(\lambda, \mathbf{s}, -\mathbf{s}')\rangle_{\Omega_i} + \langle I_d(\lambda, \mathbf{s}')p(\lambda, \mathbf{s}, \mathbf{s}')\rangle_{2\pi}\rangle_{\Omega_c}, \quad (2)$$

where $I_i(\lambda, \mathbf{s})$ is the intensity of the incident light delivered in solid angle Ω_i, $I_d(\lambda, \mathbf{s})$ is the intensity of the light emerging from the underlying tissue, and $\langle f(\mathbf{s}, \mathbf{s}')\rangle_\Omega = \int_\Omega f(\mathbf{s}, \mathbf{s}')\, d\mathbf{s}'$ for any function f and solid angle Ω, where $\mathbf{s}$ is a unit vector pointing outward from the tissue surface in an arbitrary direction. The quantity $\overline{R}(\lambda) = \langle I_d(\lambda, \mathbf{s})\rangle_{\Omega_c}/\langle I_i(\lambda, \mathbf{s})\rangle_{\Omega_c}$ is the reflectance of the diffusive background. The "optical distance" $\tau(\gamma) = \int_0^\infty \sigma_s(\lambda, l)N(l)\, dl$ [13] and scattering phase function $p(\lambda, \mathbf{s}, \mathbf{s}') = \frac{1}{\tau}\int_0^\infty p(\lambda, l, \mathbf{s}, \mathbf{s}')\sigma_s(\lambda, l)N(l)\, dl$ both depend on $N(l)$; for a sphere, $p(\lambda, l, \mathbf{s}, \mathbf{s}')$ is determined by Mie theory [11]. The first term in Eq. (2) describes the attenuation of the diffusive background, and the terms in brackets describe backscattering of the incident light and forward scattering of diffusive background by the epithelial cell nuclei, respectively.

For small Ω_c, the forward scattering and backscattering terms in Eq. (2) can be expanded in $\tau(\lambda)$. The forward scattering term oscillates in phase with $\tau(\lambda)$, as required by the optical theorem [12], whereas the backscattering term is out of phase. Thus, Eq. (2) shows that the epithelial nuclei introduce a periodic fine structure component into the reflectance with a wavelength dependence similar to that of the corresponding scattering cross section. Its periodicity is approximately proportional to nuclear diameter, and its amplitude is a function of the size and the number of nuclei in the epithelial layer. These quantities can be determined by analyzing the reflectance $R(\lambda)$.

To investigate the effects described by Eq. (2), elastic light scattering from normal and T84 tumor human colonic cell monolayers (10 and 15 sites, respectively) was studied. The cells, approximately 15 μm long, were affixed to glass slides in buffer solution and placed on top of a $BaSO_4$ diffusing (and highly reflective) plate. The tumor cells were grown in a confluent manner; normal cells were allowed to settle on a glass slide and the remaining nonattached cells were washed out. In both cases, the cells were densely packed. The diameters of the normal cell nuclei ranged from 5 to 7 μm, and those of the tumor cells from 7 to 16 μm. The $BaSO_4$ plate was used to simulate the diffuse reflectance from underlying tissue.

In the experiments, an optical fiber probe was used to deliver white light from a xenon arc flashlamp to the samples and collect the return reflectance signal. The probe tip, 1 mm in diameter, consisted of a central delivery fiber surrounded by six collection fibers (200 μm core fused silica, NA = 0.22, $\Omega_i = \Omega_c = \pi \mathrm{NA}^2$), all of which were covered with a 1 mm thick quartz optical shield [14].

Figures 1(a) and 1(b) show the normalized reflectance $R(\lambda)/\overline{R}(\lambda)$ from normal and T84 tumor cell samples, respectively. Distinct spectral features are apparent. For comparison, the reflectance spectrum from the $BaSO_4$ plate by itself is also shown [Fig. 1(c)]. This spectrum lacks structure and shows no prominent features.

To obtain information about the nuclear size distribution from the reflectance data, Eq. (2) needs to be inverted. The nuclear size distribution, $N(l)$, can then be obtained from the Fourier transform of the periodic component of the optical distance $\tau - \tau_0 \cong [1 - R(\lambda)/\overline{R}(\lambda)]/q$, where parameter $q \approx 0.15$ depends on the

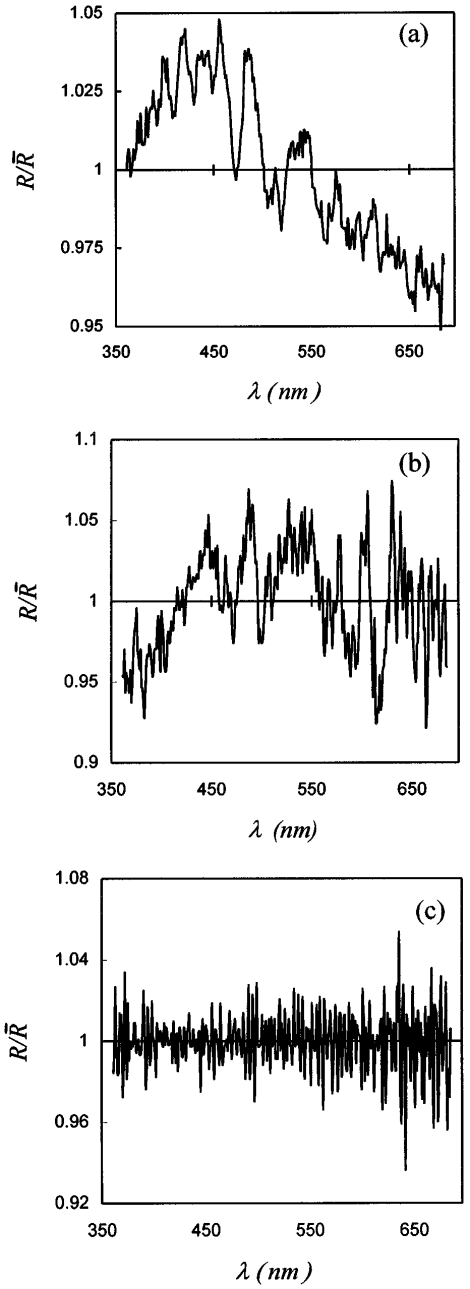

FIG. 1. Reflectance spectrum from cell monolayers. (a) Normal colon cells ($\overline{R} = 0.46$); (b) T84 cells ($\overline{R} = 0.38$); (c) $BaSO_4$ diffusing plate ($\overline{R} = 1.0$). See text for details.

probe geometry and the angular distribution of the incident and reflected light. By introducing the effective wave number $k = 2\pi n_c(n - 1)/\lambda - k_0$, we obtain

$$N(l) \cong \frac{2}{ql\pi^2} \left| \int_0^K \left(\frac{R(k)}{\bar{R}(k)} - 1 \right) e^{ikl}(k + k_0)\, dk \right|, \quad (3)$$

where $k_0 = 2\pi n_c(n - 1)/\lambda_{\max}$ and $K = 2\pi n_c(n - 1)(\lambda_{\min}^{-1} - \lambda_{\max}^{-1})$.

Equation (3) was used to analyze the data. In order to remove spurious oscillations, $N(l)$ was further processed by convolving it with a Gaussian filtering function. The solid curves of Figs. 2(a) and 2(b) show the resulting nuclear size distributions of the normal and T84 cell monolayer samples extracted from the spectra of Figs. 1(a) and 1(b). A nucleus-to-cytoplasm relative refractive index of $n = 1.06$ and cytoplasm refractive index of $n_c = 1.36$ were used. The dashed curves show the corresponding size distributions measured morphometrically via light microscopy [15]. The extracted and measured distributions are in good agreement for both normal and T84 cell samples, indicating the validity of the above physical picture and the accuracy of our method of extracting information.

We have observed this periodic fine structure in diffuse reflectance from esophagus and colon mucosa of human subjects undergoing gastroenterological endoscopy procedures. We consider here the case of Barrett's esophagus, a chronic condition in which irritation transforms normal esophagus epithelium into a thin monolayer of columnar cells similar to those used in the cell culture experiments. Such patients have an increased risk of developing dysplastic change, but such change is not visible with an endoscope.

Data were collected as in the cell culture studies. The optical fiber probe was inserted into the biopsy channel of the endoscope and brought into contact with the tissue surface. The fine structure component, which is the scattering signature of the cell nuclei, is typically less than 5% of the total signal and is ordinarily masked by the background of diffusely scattered light from underlying tissue, which itself exhibits spectral features due to absorption and scattering [Fig. 3(a)]. Its spectral features are dominated by the characteristic absorption bands of hemoglobin and scattering of collagen [16]. In order to observe the fine structure, this background must be removed using an appropriate model. The absorption length μ_a^{-1} ranges from 0.5 to 250 mm as the wavelength is varied, and the effective scattering length $(\mu_s')^{-1}$ ranges from 0.1 to 1 mm [3]. Thus, both scattering and

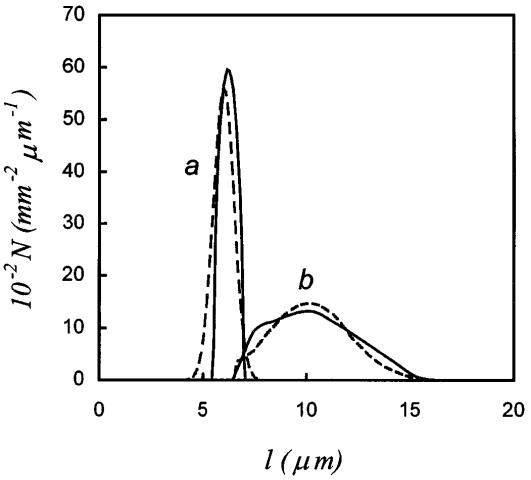

FIG. 2. Nuclear size distributions from data of Fig. 1. (a) Normal colon cells; (b) T84 cells. In each case, the solid line is the distribution extracted from the data, and the dashed line is the distribution measured using light microscopy.

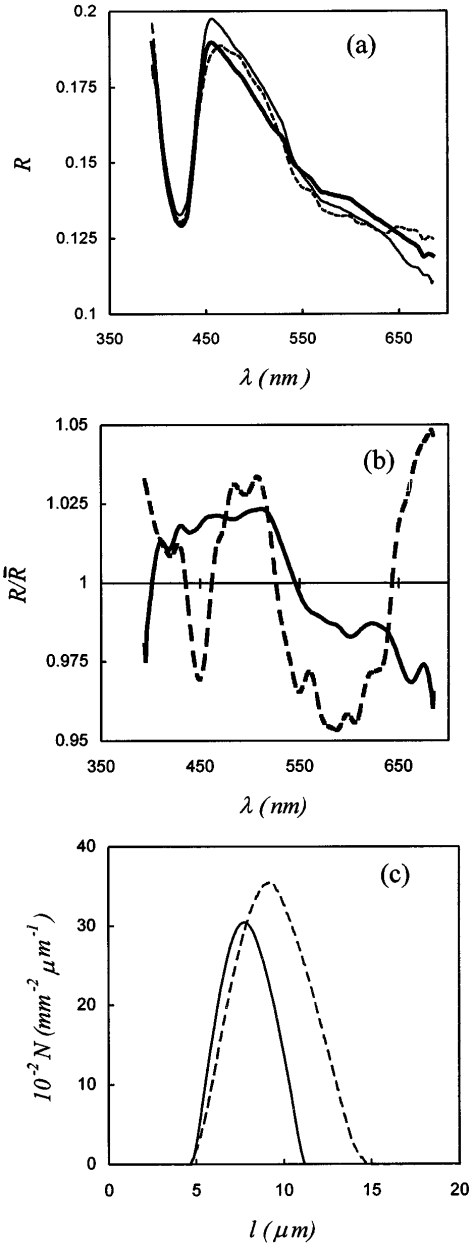

FIG. 3. Reflectance from Barrett's esophagus. (a) Diffuse reflectance from a nondysplastic site (solid line), a dysplastic site (dashed line), and the model fit (thick solid line); (b) corresponding fine structures; (c) resulting nuclear size distributions.

absorption have to be taken into account in modeling the background signal.

We employed a simple physical model to describe this background. Light incident on the tissue is assumed to be exponentially attenuated, and that, at any given depth z, an amount of light proportional to the reduced scattering coefficient $\mu_s'(\lambda)$ is scattered back towards the surface and further exponentially attenuated. Since light attenuation depends on both scattering and absorption, the attenuation coefficient is assumed to be the sum of the absorption coefficient $\mu_a(\lambda)$ and an effective scattering coefficient $\mu_s^{(e)}(\lambda) = \beta\mu_s'(\lambda)$. The parameter β was determined by comparison with Monte Carlo simulations and more accurate models of light transport, and was found to be $\beta \cong 0.07$ [1,17]. Since light only penetrates $\sim$1 mm into the tissue, most of the diffusely scattered return light is confined to the mucosal layer. The following approximate expression for the diffusive light from underlying tissue impinging on the epithelial cell layer is then obtained [7]:

$$I_d(\lambda, \mathbf{s}) = F(\mathbf{s})\langle I_i(\lambda, \mathbf{s})\rangle_{\Omega_i} \frac{1 - \exp[-(\mu_s^{(e)} + c\mu_a)L]}{1 + c(\mu_a/\mu_s^{(e)})}, \quad (4)$$

where function $F(\mathbf{s}) = \frac{\Delta + (\mathbf{s}\cdot\mathbf{n})}{\pi(2\Delta+1)}$ describes the angular dependence of light emerging from the mucosal layer, $\mathbf{n}$ is a unit vector normal to the surface of the tissue, $\Delta = 0.7104$ [18], L is a parameter representing the thickness of the mucosal layer, and c is the relative concentration of hemoglobin. Because both oxygenated and deoxygenated hemoglobin are present, the total hemoglobin absorption is modeled as $\mu_a = (1 - \alpha)\mu_a^{(\mathrm{Hb})} + \alpha\mu_a^{(\mathrm{HbO_2})}$, with oxygen saturation parameter α $(0 \le \alpha \le 1)$.

Figure 3(a) shows the reflectance spectra from two Barrett's esophagus tissue sites, independently diagnosed by two expert pathologists as nondysplastic (solid line) and dysplastic (dashed line), respectively. As can be seen, the differences in these unprocessed spectra are small. To analyze them, Eq. (4) was first fit to the broad features of the data by varying the parameters c, a, and L. As seen in Fig. 3(a), the resulting fits are quite accurate. After removing this coarse structure by calculating $R(\lambda)/\overline{R}(\lambda)$, the periodic fine structure is seen clearly [Fig. 3(b)]. Note that the fine structure from the dysplastic tissue site exhibits higher frequency content than that from the nondysplastic site. Equation (3) was then employed to extract the respective nuclear size distributions, yielding Fig. 3(c). As can be seen, the difference between nondysplastic and dysplastic tissue sites is pronounced. The distribution of nuclei from the dysplastic site is much broader than that from the nondysplastic site and the peak diameter is shifted from $\sim$7 mm to $\sim$10 mm. In addition, both the relative number of large nuclei ($>$10 mm) and the total number of nuclei are significantly increased. We further note that the method provides a quantitative measure of the density of nuclei close to the mucosal surface. These findings have been confirmed in a multipatient study, the results of which will be published elsewhere.

The ability to measure nuclear size distribution *in vivo* has valuable applications in clinical medicine. Enlarged nuclei are primary indicators of cancer, dysplasia, and cell regeneration in most human tissues. In addition, measurement of nuclei of different sizes can provide information about the presence of particular cells, and can thus serve, for example, as an indicator of inflammatory response of biological tissue. This suggests that different morphology/pathology at the mucosal surface will give rise to distinct patterns of nuclear size distributions. Additional studies are necessary to correlate the results of this work with pathology findings.

We thank D. Menemenlis for fruitful discussions. This work was supported by NIH Grants No. P41RR02594 and No. CA53717.

[1] L. T. Perelman, J. Wu, I. Itzkan, and M. S. Feld, Phys. Rev. Lett. **72**, 1341 (1994).
[2] M. A. O'Leary, D. A. Boas, B. Chance, and A. G. Yodh, Phys. Rev. Lett. **69**, 2658 (1992).
[3] A. G. Yodh and B. Chance, Phys. Today **48**, No. 3, 34 (1995).
[4] M. R. Melamed, T. Lindmo, and M. L. Mendelsohn, *Flow Cytometry and Sorting* (Wiley-Liss, New York, 1990).
[5] J. R. Mourant, T. Fuselier, J. Boyer, T. M. Johnson, and I. Bigio, Appl. Opt. **36**, 949 (1997).
[6] P. D. Kaplan, A. D. Dinsmore, A. G. Yodh, and D. J. Pine, Phys. Rev. E **50**, 4827 (1994).
[7] G. Zonios, L. T. Perelman, V. Backman, R. Manoharan, J. Van Dam, and M. S. Feld (to be published).
[8] R. S. Cotran, S. L. Robbins, and V. Kumar, *Robbins Pathological Basis of Disease* (Saunders, Philadelphia, 1994).
[9] J. Beuthan, O. Minet, J. Helfmann, M. Herrig, and G. Muller, Phys. Med. Biol. **41**, 369 (1996).
[10] P. M. A. Slot, A. G. Hoekstra, and C. G. Figdor, Cytometry **9**, 636 (1988).
[11] H. C. van de Hulst, *Light Scattering by Small Particles* (Dover, New York, 1957).
[12] R. G. Newton, *Scattering Theory of Waves and Particles* (McGraw-Hill, New York, 1969).
[13] A. Ishimaru, *Wave Propagation and Scattering in Random Media* (Academic Press, Orlando, 1978).
[14] J. F. Brennan, G. I. Zonios, T. D. Wang, R. P. Rava, G. B. Hayes, R. R. Dasari, and M. S. Feld, Appl. Spectrosc. **47**, 2081 (1993).
[15] Because of insufficient morphometric data, the nuclear size distribution for the normal cell culture sample of Fig. 2 is depicted as a Gaussian distribution with mean diameter and standard deviation determined from the light microscopy measurements.
[16] G. I. Zonios, R. M. Cothren, J. T. Arendt, J. Wu, J. Van Dam, J. M. Crawford, R. Manoharan, and M. S. Feld, IEEE Trans. Biomed. Eng. **43**, 113 (1996).
[17] J. Wu, M. S. Feld, and R. P. Rava, Appl. Opt. **32**, 3585 (1993).
[18] P. M. Morse and H. Feshbach, *Methods of Theoretical Physics* (McGraw-Hill, New York, 1953).